

Structure and Vibrational Spectroscopy of Salt  
Water/Air Interfaces: Predictions from Classical  
Molecular Dynamics Simulations

Eric C. Brown,<sup>1</sup> Martin Mucha,<sup>2</sup> Pavel Jungwirth<sup>2</sup> and Douglas J. Tobias<sup>1\*</sup>

<sup>1</sup>Department of Chemistry, and

Environmental Molecular Sciences Institute,

University of California, Irvine

Irvine, California 92697-2025, USA

and

<sup>2</sup>Institute of Organic Chemistry and Biochemistry, and

Center for Complex Molecular Systems and Biomolecules,

Academy of Sciences of the Czech Republic

Flemingovo nam. 2, 16610 Prague 6, Czech Republic

\*To whom correspondence should be addressed: dtobias@uci.edu

## Abstract

We report the Sum Frequency Generation (SFG) spectra of aqueous sodium iodide interfaces computed with the methodology outlined by Morita and Hynes (*J. Phys. Chem. B* **2002**, *106*, 673), which is based on molecular dynamics simulations. The calculated spectra are in qualitative agreement with experiment. Our simulations show that the addition of sodium iodide to water leads to an increase in SFG intensity in the region of  $3400\text{ cm}^{-1}$ , which corresponds to an increase in ordering of hydrogen-bonded water molecules. Depth-resolved orientational distribution functions suggest that the ion double layer orders water molecules which are about one water layer below the Gibbs dividing surface. We attribute the increase in SFG intensity to these ordered subsurface water molecules which are present in the aqueous sodium iodide/air interfaces, but are absent in the neat water/air interface.

# 1 Introduction

Aqueous aerosols and other particulate matter play an important role in the various chemical reactions which occur in the atmosphere. In the marine boundary layer aqueous sea-salt aerosols are ubiquitous. [1] The bursting of air bubbles trapped by wave action produces fine aerosols that are comprised primarily of alkali and alkaline earth halide salts dissolved in water. These salt water aerosols serve as a source of reactant and as a substrate for various heterogeneous reactions with polluting gases.

An example is the production of molecular chlorine via the oxidation of chloride by hydroxyl radical. In an aerosol chamber, Knipping *et al.* monitored the appearance of chlorine and the disappearance of ozone (from which hydroxyl radical was generated by photolysis in the presence of water vapor), and sought to deduce the reaction mechanism(s) by fitting their kinetic data to a sizable battery of known bulk aqueous phase chemical reactions and their respective rates. [2] This particular modeling attempt based on bulk phase chemistry failed to predict the observed production of molecular chlorine under the conditions of the experiment.

Molecular dynamics (MD) simulations predicted that heavier halides may exist at interfaces in surprisingly high abundance. [3, 4, 5, 6] The results of the MD simulations suggested that the interface can be rich in reactant chloride, and it is essential to take this into account when proposing a kinetic model that could match experimental data. [2] Indeed, when the aforementioned experimental results were analyzed using an interfacial mechanism that took into account the fact that ions could be present at interfaces,

the kinetics data were well-reproduced. [2] Hydroxide anions, predicted to be a product of the interfacial reaction, were subsequently detected in NaCl aerosol particles following exposure to hydroxyl radical. [7]

The results of the MD simulations are supported by the fact that experimental and theoretical studies on small clusters (e.g.,  $(\text{H}_2\text{O})_6\text{Cl}^-$ ) reveal that the halide ions are not completely solvated by water molecules, but instead exist in configurations where a large portion of the halide ion is exposed. [8] In contrast, similar studies on small clusters with alkali cations (e.g.  $(\text{H}_2\text{O})_6\text{Na}^+$ ) reveal that the cations are almost totally encapsulated by coordinating water molecules. [9]

The notion that atomic ions exist at the interface in surfactant-like excess is seemingly inconsistent with a straightforward application of the Gibbs adsorption relation. If, in accord with experiment and surface electrolyte theory, the surface tension of a salt solution increases relative to that of pure water, then the concentration of solute (in this case, the ions) must decrease at the interface. For example, the surface tension of 1 M NaI in water is higher by roughly 1% than that of pure water, [10] so one might deduce that there should be fewer ions at the interface than in the bulk. However, as we have recently discussed, [11] this behavior can also be rationalized in terms of a non-monotonous ionic density profile with surface enhancement and subsurface depletion, with a different behavior of cations and anions at the interface.

A simple explanation for the observation that cations and anions associate differently at the air/water interface is that the halide anions are, except for fluoride, more polarizable and larger than the alkali cations and even water molecules. Qualitatively speaking, the

electron clouds of the polarizable anions can easily be distorted by the non-vanishing electric field at the interface which can make the surface location favorable. [11]

Due to their surface specificity, nonlinear spectroscopies [12, 13] such as Sum Frequency Generation (SFG) spectroscopy [14, 15] are becoming important tools for elucidating molecular structure at solid and liquid surfaces.[13] The surface specificity derives from the fact that the signal averages to zero in centrosymmetric environments. The SFG spectrum of the pure water/air interface has been known for almost a decade,[13] and recently, the SFG spectra of the series of sodium halide/air interfaces have been measured over a range of frequencies spanning the water OH stretching region. [16, 17]

The SFG spectrum of pure water is different than the SFG spectra of some of the salt water/air interfaces (e.g., aqueous NaI); hence, one may conclude that the interfaces are different from a structural and/or dynamical point of view. However, there remains uncertainty as to whether these salt water SFG spectra correspond to an environment where some ions exist at the surface in a surfactant-like way (as predicted by classical MD simulations) or whether these spectra correspond to an environment where the interface is perhaps only slightly perturbed by the presence of ions in the subsurface. Thus, the spectra alone have not provided a definitive answer to the question raised by MD simulations: is the concentration of ions such as iodide or bromide in certain regions of the air/water interface higher than the concentration of the salts in the bulk?

The above-mentioned experimental studies of sodium halide water interfaces which include SFG spectra for the entire sodium halide series revealed that trends in spectral features are enhanced upon moving down the periodic table. [16, 17] A similar trend is

readily apparent from MD simulations of 1.2 M solutions of NaF, NaCl, NaBr, and NaI, which showed that the probability of finding a halide anion at the interface increased in the order  $F^- < Cl^- < Br^- < I^-$ . [3] Indeed, this is the trend that one would predict based on the fact that the halide polarizability and ion size increase in the same manner. It is also important to point out that when, in computational experiments based on MD simulations, the particles are prevented from undergoing polarization (i.e., their polarizability parameters are set to be zero), the anions to a large extent lose their tendency to exist at the surface; and, except for the heaviest halides, they are repelled from the interface in accord with the classical theory of electrolyte surfaces. [3] Variation of the polarizability parameters allows us to generate molecular dynamics configurations where the ion distribution ranges from being surfactant-like to a situation where the ion distribution is more like that of the bulk solution. [11]

Of all the sodium halides, the SFG spectrum of sodium iodide (NaI) in water exhibits the largest differences from the SFG spectrum of neat water. The main goal of this work was to compute the SFG spectrum of the aqueous sodium iodide interface from molecular dynamics simulations. Comparison of available experimental SFG spectra [16, 17] with our computed spectra, in conjunction with the structures provided by MD simulations, will enable us to determine whether or not ion adsorption to the air-water interface is manifested in the spectra and, if so, to elucidate the molecular origins of the spectral changes.

## 2 Computational Methodology

Although other methods for computing SFG spectra exist, [18, 19, 20, 21] a straightforward and general way to predict SFG spectra is via time correlation functions computed from classical molecular dynamics trajectories. Morita and Hynes have outlined such a procedure, and the reader is referred to their particularly lucid work [22] for the derivations of the expressions outlined in this section. Here, we adopt their notation and describe only the essential steps that we took in order to obtain the theoretical spectra reported in this work. While Morita and Hynes have successfully treated the neat water interface with this procedure, we emphasize that we shall focus on *differences* between neat water and salt water solutions computed in a similar way.

Most of the reported experimental investigations of (salt) water interfaces have employed the *ssp* light polarization. [13, 16, 17] The SFG lineshape ( $I_{xxz}$ ) for this particular polarization is given as:

$$I_{ssp} \propto \left( \frac{\omega_{IR} + \omega_{vis}}{\omega_{IR}} \right)^2 |\chi_{xxz}|^2 \quad (1)$$

where  $\omega_{IR}$  and  $\omega_{vis}$  are the frequencies of the incident infrared and visible radiation, respectively,  $\chi_{xxz}^R$  is the second-order nonlinear susceptibility, and  $x$  and  $z$  are Cartesian coordinates parallel and normal, respectively, to the interface.

$\chi_{xxz}$  is a complex quantity, being the sum of a complex resonant term,  $\chi_{xxz}^R$ , and a real nonresonant term,  $\chi_{xxz}^{NR}$ , that depends on the sum of the molecular hyperpolarizabilities ( $\beta$ ):

$$\chi_{xxz}^R = i \int_0^\infty \langle A_{xx}(t) M_z(0) \rangle e^{i\omega t} dt \quad (2)$$

$$\chi_{xxz}^{NR} = \frac{1}{2} \left\langle \sum_i^{\text{molecules}} \beta_{xxz}(i) \right\rangle \quad (3)$$

where  $A_{xx}$  and  $M_z$  are components of the system polarizability tensor and dipole moment, respectively. [13, 18] Since on long time scales the  $x$  and  $y$  dimensions are equivalent for a planar interface (i.e. axial symmetry),  $A_{yy}$  and  $M_z$  also represents a valid combination for describing the SFG intensity  $I_{sfp}$ , and we average contributions from the  $x$  and  $y$  directions for all of the SFG spectra reported in this work.

It is the resonant part ( $\chi_{xxz}^R$ ) of the total susceptibility that gives rise to the features that dominate the corresponding SFG spectrum. The quantities  $A$  and  $M$  are represented as the sum of the molecular quantities at each time step of the MD simulation:

$$A(t) = \sum_i^{\text{molecules}} \alpha_i(t) \quad (4)$$

$$M(t) = \sum_i^{\text{molecules}} \mu_i(t) \quad (5)$$

where  $\alpha_i(t)$  is the polarizability tensor of an individual molecule  $i$  at time  $t$ , and  $\mu_i(t)$  is the dipole moment of an individual molecule at time  $t$ .

These simulations must be performed with a flexible force-fields, i.e. water molecules must be free to undergo stretching and bending motion. At each instantaneous molecular position, the dipole moment and polarizability for each molecule is determined from *ab initio* data. Specifically, each water molecule is rotated from its laboratory frame orientation into a standard orientation, where the properties are mapped onto functions representing the center of charge, dipole, polarizability, and hyperpolarizability. These functions were determined by fitting *ab initio* values at various grid points computed at the B3LYP/d-



aug-cc-pVDZ level of theory [23, 24, 25, 26, 27] with the Gaussian 03 suite of programs. [28] Whereas Morita and Hynes represented these molecular quantities via O-H bond additivity, we chose to represent the dipole functions over the internal coordinate space of the entire molecule. Since at the grid point geometries both our treatment and theirs [22] yield fitted values that are virtually identical to the ab initio quantities, we conclude that these two approaches are equivalent for water. [29, 30, 31] These interpolated quantities enter into the summations in eqs 4 and 5. Note that the mapping is done using configurations generated by MD simulations based on empirical force fields.

The flexible, SPC/E-like water potential of Ferguson [32] was chosen for this study because it has previously shown to reproduce the experimental SFG spectrum of neat water reasonably well. [22] For the ions, the polarizable potentials for sodium and iodide of Markovich et al. were employed. [33] All of the MD simulations were performed with the *AMBER 7* [34] suite of programs, modified in-house to implement the cubic (anharmonic) O-H stretch terms required by the Ferguson model. The dimensions of the prismatic unit cell were chosen to be 30 Å in the  $x$  and  $y$  dimensions and 160 Å in the  $z$  dimension, resulting in a slab geometry with two solution/vapor interfaces. Particle-Mesh Ewald summation was performed in order to account for long-range electrostatic effects. [35] Initial configurations for the trajectories were taken from evenly-spaced snapshots from a previous 1 ns molecular dynamics simulation. [4] Systems containing pure water had 864 molecules and systems containing water and ions had 864 waters, 18 cations, and 18 anions, giving 1.2 M NaI solutions. The initial velocities for each configuration were randomly sampled from a Maxwellian distribution corresponding to 300 K.

The first studies of aqueous salt-water interfaces that employed polarizability in the molecular dynamics force fields considered polarization effects on the ions and on the waters.[36, 4, 5, 6] In those studies, the water molecules had rigid O-H bonds, whereas in this study, the O-H bonds were allowed to undergo vibration. Because the simultaneous incorporation of polarizability, flexibility of the water O-H bonds, and a lack of a Lennard-Jones repulsion term for hydrogen leads to the well-known “polarization catastrophe,” [37, 38] we were not able to augment the Ferguson model of water with the atom-based polarizability model as implemented in *AMBER 7*. Nevertheless, as we have previously shown, [11] most of the surface excess of ions like iodide can be obtained using force fields with polarizability only on the ions and a non-polarizable water molecules[11], and hence this is the treatment also adopted in this work.

For the SFG modelling, following Morita and Hynes,[22] for each of the runs we chose a 0.6 fs time step and performed equilibration for 15 ps with the Berendsen thermostat, followed by a 15 ps acquisition time in the NVE ensemble. From these latter trajectories, the time-dependent system dipole and polarizability were evaluated with the inclusion of the local field corrections. We removed the effect of rotational drift on this short time scale by smoothing the resulting  $M(t)$  and  $A(t)$  with a broad Gaussian function, and then subtracting this result from the initial values in order to obtain  $M(t)$  and  $A(t)$  solely as a result of water vibrational motions.

A simple sum over the permanent gas-phase dipole moments and polarizabilities is only an approximate description of the system dipole and polarizability. It neglects several important factors: 1) the condensed phase effect on molecular properties, 2) the fact that

the interfacial region is a different chemical environment than the bulk phase, and 3) the fact that the interaction of a water molecule with a nearby ion is likely to be strong. To account for these effects, each of the dipole moments and polarizabilities were corrected with a many-body approach. [22, 39, 40]

Eq 6 and 7 represent the simultaneous linear equations which must be solved in order to correlate the dipoles and charges for each MD configuration:

$$(\mathbf{1} + \mathbf{T}\alpha)\mathbf{E} = \mathbf{E}^{\text{cd}} - \mathbf{T}\mathbf{p}^0 \quad (6)$$

$$(\mathbf{1} + \mathbf{T}\alpha)\mathbf{f} = \mathbf{h} \quad (7)$$

where  $\mathbf{T}$  is the dipole field tensor,  $\alpha$  is a polarizability matrix,  $\mathbf{E}^{\text{cd}}$  is the term which accounts for the field due to the permanent charges on the dipoles,  $\mathbf{p}^0$  is the polarization (dipole moment) vector,  $\mathbf{f}$  is a local field correction, and  $\mathbf{h}$  is a vector of identity matrices. The linear equations describing the effects of induced polarization [22] were solved iteratively with the GMRES algorithm.[41] The construction and solution of these equations accounts for the vast majority of the time required to perform the spectral calculations.

The perturbed molecular dipole moments and polarizabilities from eqs 8 and 9 below are then used in eq 2 in place of the gas phase values (eqs 4 and 5): according to

$$A(t) = \sum_i^{\text{molecules}} \alpha_i(t) \cdot f_i(t) \quad (8)$$

$$M(t) = \sum_i^{\text{molecules}} \mu_i(t) + \alpha_i(t)E_i(t) \quad (9)$$

and the nonresonant susceptibility is modified as:

$$\chi_{xxz}^{NR} = \frac{1}{2} \left\langle \sum_i^{\text{molecules}} \sum_{q,r}^{x-z} \beta_{xxz}(i) f_{qx}(i) f_{rz}(i) \right\rangle \quad (10)$$

While we expect that the actual vibrational frequencies depend mostly on the chemical environments that arise from the molecular dynamics force field, the intensities of these transitions are affected by the magnitudes of the dipole moments and polarizabilities which enter eq 2. [22] While the average dipole moment of a gas phase water molecule is 1.8 D (taken from the B3LYP calculations, in excellent agreement with experiment [42]), the most probable dipole moment in these systems, after application of eqs 8 and 9, is 2.2 D, which is closer to the *ab initio* estimate for liquid water of about 2.6 D. [43] In this work, we also make use of an *ab initio*-deduced gas-phase polarizability of the iodide ion of 6.9 Å<sup>3</sup>, and the sodium polarizability was similarly chosen to be 0.24 Å<sup>3</sup>.

Since these slabs possess two interfaces (“top” and “bottom”), averaging may be performed over both. However, straightforward summation over the entire slab would lead to the cancellation of surface normal components since the two interfaces “point” in opposite directions. Therefore, one must choose one interface to have the positive normal direction, and appropriately reflect the other interface such that its normal direction is the same as the other. At the beginning of each trajectory, the molecules were assigned to a particular interface for the duration of the 15 ps run, and were counted as being in a particular slab side when accumulating properties.

Correlation functions were computed using the Wiener-Kinchin method. [44] The resulting correlation functions were exponentially damped with a damping constant of 0.0025

ps<sup>-1</sup>. Lastly, the Fourier transform of each damped correlation function yields the corresponding frequency spectrum. During the course of the calculation of an SFG spectrum, we may readily compute the infrared and Raman spectra since they are related to the Fourier transforms of the appropriate autocorrelation functions,  $\langle M(0) \cdot M(t) \rangle$  and  $\langle \text{Tr}[A(0) \cdot A(t)] \rangle$ , respectively. [45, 46]

Spectral convergence was assessed by comparing the average results of the top of the slab to the average results from the bottom of the slab. The resonant susceptibilities of each of the systems considered herein were well-converged in 128 trajectories.

In addition to computed SFG spectra, we report the results of several standard structural diagnostics. Density profiles and orientational distribution functions of the angle bisector of each water molecule with respect to the surface-normal direction were computed. Dangling OH bonds were defined as those not acting as hydrogen bond donors, with hydrogen bonds defined by using a geometric criterion: the oxygen atom of a potential hydrogen bond donor is less than 3.5 Å from the oxygen on a potential hydrogen bond acceptor, and the angle between the donor hydrogen, donor oxygen, and acceptor oxygen is less than 30° (Figure 1).

### 3 Results and Discussion

First, we characterize the various systems by analyzing the structures obtained from the molecular dynamics simulations; and, subsequently, we report predictions of the IR, Raman, and SFG spectra. We consider three systems: 1) neat water (NEAT), 2) 1.2 M

sodium iodide in water with polarizable ions (IPOL), and 3) a system analagous to IPOL, but with the polarizabilities “switched off” (INP). As expected, the ion distribution for IPOL is surfactant-like for iodide, with the sodium ions broadly peaking in the subsurface. The ion distribution for INP is more homogeneous, although it does exhibit a small surface anion enhancement (Figure 2). [11]

### 3.1 Structure

As stated in the introduction, we aim to resolve, from structural and spectroscopic considerations, how changes in the SFG spectrum correlate with the presence of halide ions near the air/water interface. SFG spectroscopy, within the dipolar approximation, gives intensities corresponding to oscillators that are in anisotropic environments. Therefore, it is reasonable to begin this discussion by identifying which regions in the slab correspond to such environments. A convenient way to visualize this anisotropy is to plot the orientational distribution function (ODF) of the water dipole moments (i.e., the distribution of angles between the H-O-H angle bisector and the surface normal vector). At the Gibbs dividing surface ( $Z=0$  Å), the ODF of the neat water system (NEAT) has a maximum corresponding to an angle of  $\sim 78^\circ$  (Figure 3), which is in good agreement with the value obtained by Benjamin for SPC/E water (upon which the Ferguson model is based). [46, 47]

Figure 3 also shows the ODFs of IPOL and INP systems, respectively. Despite the fact that in IPOL there is an appreciable ion concentration at the surface, the largest difference (Figure 4) between neat water and IPOL and between neat water and INP is

in the region 4-5 Å below the Gibbs dividing surface. In this subsurface region, the ODF difference plots (Figure 4) reveal that in IPOL and INP there is a significant ordering of waters corresponding to an angle of  $\sim 0^\circ$  between the water dipole moments and the surface normal vector. We speculate that this (time-averaged) ordering is due to the separation of anions and cations in the interfacial layer. This conclusion is supported by the fact that a greater subsurface water ordering is found in the case of IPOL than in the case of INP (Figure 4), coupled with the fact that the density profile of IPOL exhibits a more pronounced ion double-layer than does that of INP (Figure 2). At this concentration (1.2 M and a roughly 2.5 M effective peak surface ion concentration in IPOL), it is likely that the water ordering by the ions is largely local in nature. That is, the orientation of the water molecules is caused by interaction with at most one anion and one cation, rather than caused by an electric field more akin to a capacitor model.

Comparison of the ODFs of the three systems does not reveal a large difference between NEAT, IPOL, and INP in water orientation at the Gibbs dividing surface. Water molecules in this region give rise to the so-called “dangling O-H” or “free O-H” band in the SFG spectrum (ca.  $3750\text{ cm}^{-1}$ , *vide infra*).<sup>[48]</sup> Because the SFG spectrum depends significantly on the number density of oscillators of this type, it is useful to compare the number of molecules which contain free O-H bond between each of the systems. As is evident in Figure 5, there are no large differences, and hence one would not expect there to be large differences in the SFG spectra due to a change in number density of free O-H oscillators.

## 3.2 Spectroscopy

As a way of highlighting the usefulness of SFG spectroscopy, we begin the discussion of our spectroscopic calculations by demonstrating the limitations of IR and Raman spectroscopies for differentiating between the salt water solutions and the neat water system. Because the SFG intensity arises from the quantities also required to compute the IR and Raman spectra,[45] the latter are readily computed during the course of the computation of the SFG spectrum.

Linear spectroscopies (e.g., IR and Raman) give rise to features corresponding to both bulk and interfacial waters (i.e., isotropic and anisotropic environments). As expected, there is almost no difference between the theoretical IR (Figure 6) or Raman (Figure 7) spectra of the NEAT, IPOL and INP systems. Benjamin has pointed out that hypothetical IR spectra of only the top-most layer can be calculated.[46] We also report these theoretical, top-most layer IR and Raman spectra for each of the systems in Figures 6 and 7. These spectra yield two important details: 1) the appearance of the “free O-H” oscillator as a shoulder at ca.  $3750\text{ cm}^{-1}$  and 2) the fact that there is only a small difference between the IR and Raman spectra in terms of the relative intensities of the hydrogen bonded region and the “free O-H” region. We conclude from these spectra that there is either not much difference between the oscillators of the different systems, or that the spectral differences between NEAT, IPOL, and INP are masked by bulk-like contributions.

In contrast to the linear spectroscopies, in SFG spectroscopy, bulk-like contributions vanish, leaving only the anisotropic environments more clearly visible in the spectrum. The



computation of SFG spectra involves a large amount of sampling over many trajectories in order to average the bulk-like components to zero. [22] Since these calculations are rather time consuming, it is desirable to find a way to reduce the required effort. The ODFs give some clue as to which regions of the bulk are anisotropic and which are isotropic. The computed susceptibilities converge at about  $Z=9 \text{ \AA}$ , where the ODF profiles strongly suggest that the environment is isotropic. Therefore, the computed susceptibilities and SFG spectra involve summation of molecules which are no more than  $9 \text{ \AA}$  below the Gibbs dividing surface.

The resonant susceptibilities of NEAT, IPOL, and INP are similar in the region around  $3750 \text{ cm}^{-1}$  (Figure 8). However, the salt water solutions have a clear “onset” at  $3300 \text{ cm}^{-1}$ , which gives rise to the features in the SFG spectrum corresponding to a peak maximum of  $\sim 3400 \text{ cm}^{-1}$ . Since the main structural difference between NEAT and the salt water interfaces (INP and IPOL) is the presence of the subsurface water ordering in the latter systems, we attribute this feature to water oscillators which are ordered by the ion double layer. Unfortunately, the phase information corresponding to this feature is lost in the actual SFG spectrum, since the intensity is related to the square modulus of the susceptibility according to eq 1. [13]

The theoretical SFG spectrum given by eq 1 involves the sum of the resonant and nonresonant susceptibilities. Although we originally attempted to compute the frequency-independent nonresonant susceptibility of each system following the prescription of Morita and Hynes, the values were plagued by large statistical uncertainties and turned out to be orders of magnitude off from what would be required to generate a reasonable SFG

spectrum from the simple addition of this term to the resonant contribution.[22] Therefore, we simply chose  $\chi^{NR}$  to be a real-valued, adjustable parameter which furnishes the SFG spectra with baselines similar to the ones revealed experimentally. We investigated a range of values for this term and there appear to be bounds in which a reasonable lineshape and baseline are maintained. Whereas we are confident that the chosen values of the non-resonant term yield computed SFG spectra that are “realistic,” we point out that a weakness of this approach is that the accurate, first-principles calculation of this term remains elusive. [22]

Figure 9 shows our computed SFG spectra (*ssp* polarization) for NEAT, IPOL, and INP. The computed SFG spectra of the three systems exhibit similar features: a broad band around  $3400\text{ cm}^{-1}$  corresponding to stretching of waters in the hydrogen bonded region, and a sharp intensity at  $3750\text{ cm}^{-1}$  that corresponds to the “free O-H” stretch. Our computed SFG spectrum for neat water is in excellent agreement with that reported by Morita and Hynes for a somewhat smaller system. [22] The main difference between predicted SFG spectrum of the neat water system and the predicted spectra of the salt water systems is that in the salt water systems there is, in qualitative agreement with experiment, a considerable increase in intensity of the region around  $3400\text{ cm}^{-1}$  relative to the “free O-H” stretch in the salt water systems.

## 4 Conclusions

Based on the results of molecular dynamics simulations, we predict that iodide ions exist at the air/water interface with a surfactant-like excess. When polarizability is included in the force field of the ions (IPOL), this excess is much greater than the case where the ion polarizability is neglected (INP). This is in agreement with our previous simulations that employed a somewhat different (i.e., polarizable, rigid) model for the water molecules.

Comparison of the time-averaged orientational distribution functions of the water dipoles with respect to the surface-normal vector in IPOL and NEAT reveals that there is a significant subsurface ordering in IPOL that does not appear in the case of NEAT. Because the excess ordering corresponds to an angle of  $\sim 0^\circ$  with respect to the surface normal vector, and the depletion of ordering corresponds to an angle of  $\sim 150^\circ$ , we postulate that these deviations from time-averaged isotropic orientation are due to electrostatically favorable ( $\sim 0^\circ$ ) and electrostatically unfavorable ( $\sim 150^\circ$ ) interactions of water with a time-averaged ionic double layer. This assumption is supported by the fact that INP, which has a less-pronounced ion double layer, also shows less subsurface water ordering than IPOL.

We have computed the theoretical SFG spectra of these systems using the approach outlined by Morita and Hynes.[22] We have demonstrated that there is a significant enhancement in the SFG intensity at  $3400\text{ cm}^{-1}$  upon the addition of sodium iodide. This is in agreement with the experimental results of the groups of Richmond [17] and Allen. [16] There is no significant difference in absolute intensities in the  $3400\text{ cm}^{-1}$  region between IPOL and INP, despite the stronger ion separation and water ordering in the interfacial

layer in the former case. The increase (vs. neat water) of the intensity of the  $3400\text{ cm}^{-1}$  band relative to the  $3750\text{ cm}^{-1}$  band is slightly larger in the IPOL system compared to the INP system. Taken together, our computed spectra and structural analysis suggest that the changes in the experimentally measured SFG spectra accompanying addition of sodium iodide to water could be consistent with the adsorption of anions and the presence of a diffuse double layer at the solution-air interface, with a concomitant increase in ordering of the interfacial water molecules.

SFG spectroscopy, which directly probes the water oscillators, is an indirect probe of the presence and structure of the ions in the interfacial layer. Moreover, quantitative characterization of the water subsurface ordering (presumably caused by interaction with the interfacial ion double layer) via SFG spectroscopy might be difficult due to the fact that all phase information is lost. However, subsurface ordering is predicted to be visible in the resonant susceptibility, which does exhibit strong sensitivity to the orientation of the water molecules as manifested in the phase of this complex quantity. Shen and coworkers have recently reported experimental resonant susceptibilities for aqueous systems, although these studies involved a solid surface.[49] Alternatively, SFG spectra which employ different polarizations (e.g., *ppp*) might reveal the existence of subsurface water ordering. It would be interesting to see the results of further experiments which probe salt solution/air interfaces.

## 5 Acknowledgement

We are grateful to Prof. A. Morita, Prof. J. T. Hynes, Prof. B. J. Finlayson-Pitts, Dr. J. S. Vieceli, and Dr. J. A. Freites for fruitful discussions. The applicability of the iterative solver used in this work was demonstrated by Miss O. Mandelshtam and Prof. V. Mandelshtam. Prof. H. C. Allen and Prof. G. S. Richmond are acknowledged for providing us with their experimental SFG spectra prior to publication. All calculations were performed on the Medium Performance Cluster at the University of California. We thank the National Science Foundation (via the Environmental Molecular Sciences Institute) and the Czech Ministry of Education (grant ME644) for financial support.

## References

- [1] Finlayson-Pitts, B. J.; Pitts, J. N. *Chemistry of the Upper and Lower Atmosphere*; Academic Press: San Diego, 2000.
- [2] Knipping, E. M.; Lakin, M. J.; Foster, K. L.; Jungwirth, P.; Tobias, D. J.; Gerber, R. B.; Dabdub, D.; Finlayson-Pitts, B. J. *Science* **2000**, 288, 301.
- [3] Jungwirth, P.; Tobias, D. J. *Journal of Physical Chemistry B* **2002**, 106, 6361.
- [4] Jungwirth, P.; Tobias, D. J. *Journal of Physical Chemistry B* **2001**, 105, 10468.
- [5] Dang, L. X. *Journal of Physical Chemistry B* **2002**, 106, 10388.
- [6] Dang, L. X.; Chang, T. M. *Journal of Physical Chemistry B* **2002**, 106, 235.
- [7] Laskin, A.; Gaspar, D. J.; Wang, W.; Hunt, S. W.; Cowin, J. P.; Colson, S. D.; Finlayson-Pitts, B. J. *Science* **2003**, 301, 340.
- [8] Tobias, D. J.; Jungwirth, P.; Parrinello, M. *Journal of Chemical Physics* **2001**, 114, 7036.
- [9] Perera, L.; Berkowitz, M. L. *Journal of Chemical Physics* **1991**, 95, 1954.
- [10] Washburn, E. W. *International Critical Tables, Volume IV*; McGraw-Hill: New York, 1928.
- [11] Vrbka, L.; Mucha, M.; Minofar, B.; Jungwirth, P.; Brown, E. C.; Tobias, D. J. *Current Opinon in Colloid and Interface Science* **2004**, 9, 67.

- [12] Mukamel, S. *Principles of Nonlinear Optical Spectroscopy*; Oxford University Press: Oxford, 1995.
- [13] Shen, Y. R. . In *Proceedings of the International School of Physics "Enrico Fermi"*, Vol. 120; Hansch, T.; Ingusio, M., Eds.; North-Holland: Amsterdam, 1994.
- [14] Eisenthal, K. B. *Chemical Reviews* **1996**, *96*, 1343.
- [15] Richmond, G. L. *Chemical Reviews* **2002**, *102*, 2693.
- [16] Liu, D.; Ma, G.; Levering, L. M.; Allen, H. C. *Journal of Physical Chemistry B* **2004**, *108*, 2252.
- [17] Raymond, E. A.; Richmond, G. L. *Journal of Physical Chemistry B* **2004**, *108*, 5051.
- [18] Pouthier, V.; Hoang, P. N. M.; Girardet, C. *Journal of Chemical Physics* **1999**, *110*, 6963.
- [19] Morita, A.; Hynes, J. T. *Chemical Physics* **2000**, *258*, 371.
- [20] Brown, M. G.; Walker, D. S.; Raymond, E. A.; Richmond, G. *Journal of Physical Chemistry B* **2003**, *107*, 237.
- [21] Perry, A.; Ahlborn, H.; Space, B.; Moore, P. *Journal of Chemical Physics* **2003**, *118*, 8411.
- [22] Morita, A.; Hynes, J. T. *Journal of Physical Chemistry B* **2002**, *106*, 673.
- [23] Becke, A. D. *Journal of Chemical Physics* **1993**, *98*, 5648.

- [24] Lee, C.; Yang, W.; Parr, R. G. *Physical Review B* **1988**, *37*, 785.
- [25] Kendall, R.; T.H. Dunning, J.; Harrison, R. *Journal of Chemical Physics* **1992**, *96*, 6796.
- [26] Dunning, T. H. *Journal of Chemical Physics* **1994**, *100*, 2975.
- [27] Basis sets were obtained from the Extensible Computational Chemistry Environment Basis Set Database, Version 02/25/04, as developed and distributed by the Molecular Science Computing Facility, Environmental and Molecular Sciences Laboratory which is part of the Pacific Northwest Laboratory, P.O. Box 999, Richland, Washington 99352, USA, and funded by the U.S. Department of Energy. The Pacific Northwest Laboratory is a multi-program laboratory operated by Battelle Memorial Institute for the U.S. Department of Energy under contract DE-AC06-76RLO 1830. Contact David Feller or Karen Schuchardt for further information.
- [28] Frisch, M. J. *et al. Gaussian 03, Revision A.1* **2003**, Gaussian, Inc., Pittsburgh, PA.
- [29] Denbigh, K. G. *Transactions of the Faraday Society* **1940**, *36*, 936.
- [30] LeFevre, C. G.; LeFevre, R. J. W. *Reviews in Pure and Applied Chemistry* **1955**, *5*, 261.
- [31] Miller, K. J. *Journal of the American Chemical Society* **1990**, *112*, 8543.
- [32] Ferguson, D. M. *Journal of Computational Chemistry* **1995**, *15*, 501.



- [33] Markovich, G.; Perera, L.; Berkowitz, M. L.; Cheshnovsky, O. J. *Journal of Chemical Physics* **1006**, 105, 2675.
- [34] Case, D. A. *et al.* *AMBER 7* **2002**, University of California, San Francisco.
- [35] Essmann, U.; Perera, L.; Berkowitz, M. L.; Darden, T.; Petersen, L. G. *Journal of Chemical Physics* **1995**, 103, 8577.
- [36] Jungwirth, P.; Tobias, D. J. *Journal of Physical Chemistry B* **2000**, 104, 7702.
- [37] Thole, B. T. *Chemical Physics* **1981**, 59, 341.
- [38] van Duijnen, P. T.; Swart, M. *Journal of Physical Chemistry A* **1998**, 102, 2399.
- [39] Applequist, J.; Carl, J. R.; Fung, K.-K. *Journal of the American Chemical Society* **1972**, 94, 2952.
- [40] Silberberg, L. *Phil. Mag.* **1917**, 33, 521.
- [41] van der Vorst, H. A.; Vuik, C. *Numerical Linear Algebra Applications* **1994**, 1, 369.
- [42] Clough, S. A.; Beers, Y.; Klein, G. P.; Rothman, L. S. *Journal of Chemical Physics* **1973**, 59, 2254.
- [43] Silvestrelli, P. L.; Parrinello, M. *Physical Review Letters* **1999**, 82, 3308.
- [44] Press, W. H.; Teukolsky, S. A.; Flannery, B. P.; Vetterling, W. T. *Numerical Recipes in Fortran: The Art of Scientific Computing*; Cambridge University Press: New York, 1992.

- [45] Gordon, R. G. *Advances in Magnetic Resonance* **1968**, 3, 1.
- [46] Benjamin, I. *Physical Review Letters* **1994**, 73, 2083.
- [47] Benjamin, I. *Chemical Reviews* **1996**, 96, 1449.
- [48] Wei, X.; Shen, Y. R. *Physical Review Letters* **2001**, 86, 4799.
- [49] Shen, Y. R. Sum-frequency vibrational spectroscopy of water/quartz interfaces: Crystalline vs. fused quartz. In *Abstracts of the American Chemical Society National Meeting*; American Chemical Society: Anaheim, California, 2004.

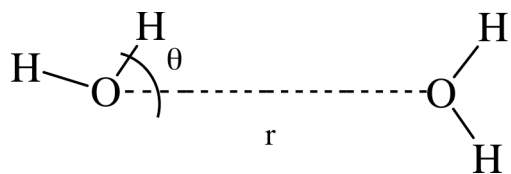


Figure 1: Schematic description of the distances and angles involved in the definition of the “free O-H” bond. The angle criterion is  $30^\circ$ , and the distance criterion is  $3.5 \text{ \AA}$ .

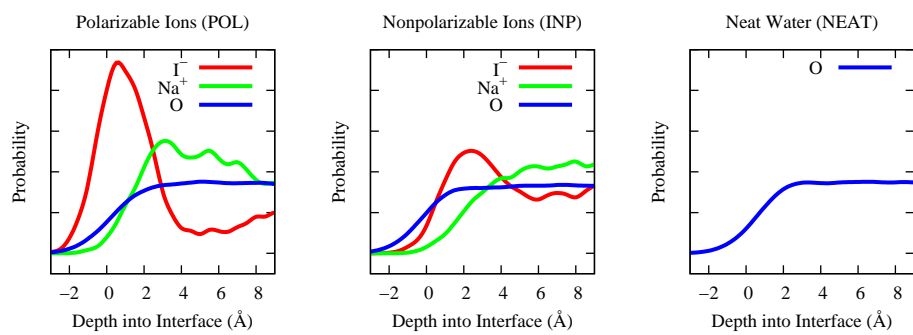


Figure 2: Density profiles of IPOL (left panel), INP (center panel), and NEAT (right panel). Zero on the x-axis corresponds to the Gibbs dividing surface.

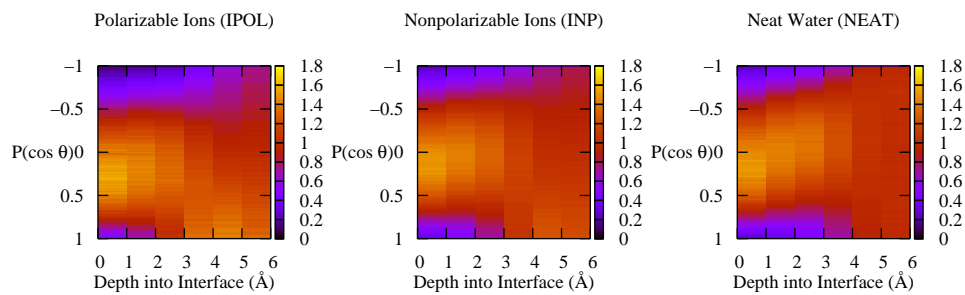


Figure 3: Orientational distribution functions as a function of depth into the interface. The values have been scaled such that a unit value corresponds to an isotropic environment.

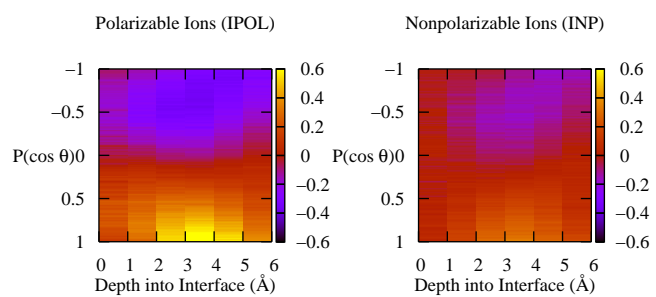


Figure 4: Orientational distribution functions of IPOL and INP, less the ODF profile of NEAT.

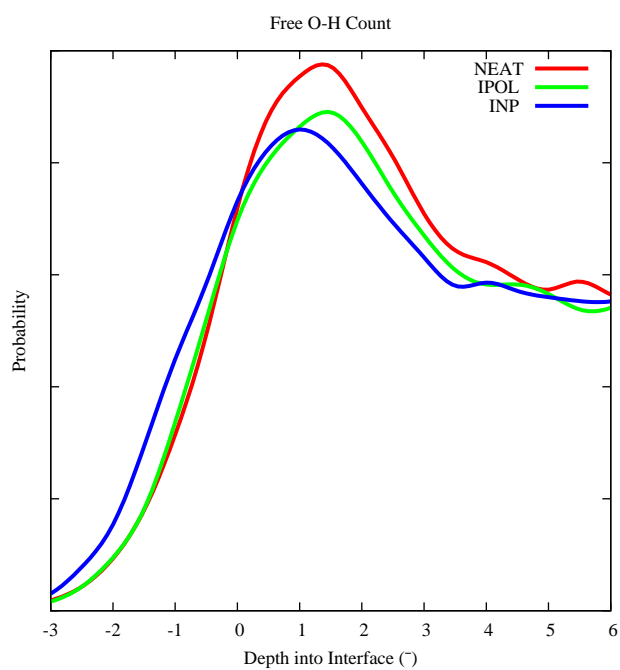


Figure 5: Number of O-H bonds characterized as being a “free O-H” bond, resolved into depth into the interface.

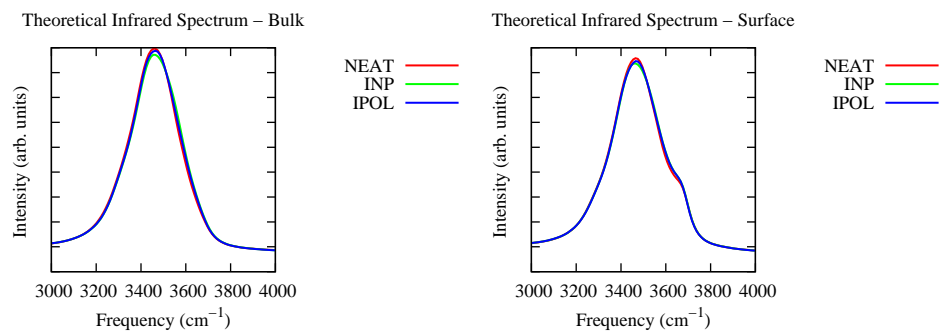


Figure 6: Theoretical infrared spectrum of the bulk (left panel) and topmost layer ( $Z < 0$ ) of IPOL, INP, and NEAT.



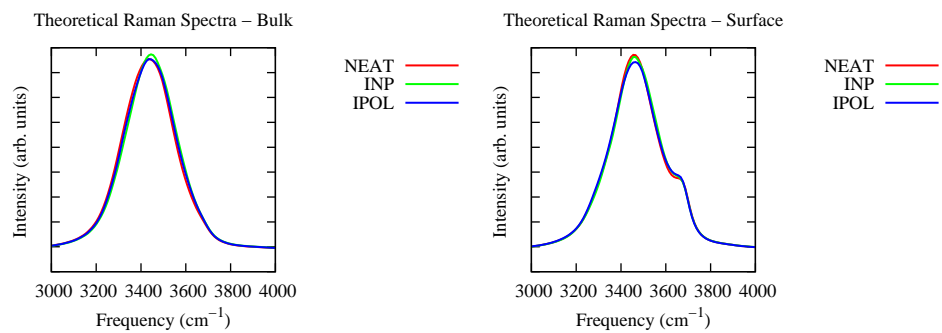


Figure 7: Theoretical infrared spectrum of the bulk (left panel) and topmost layer ( $Z < 0$ ) of IPOL, INP, and NEAT.

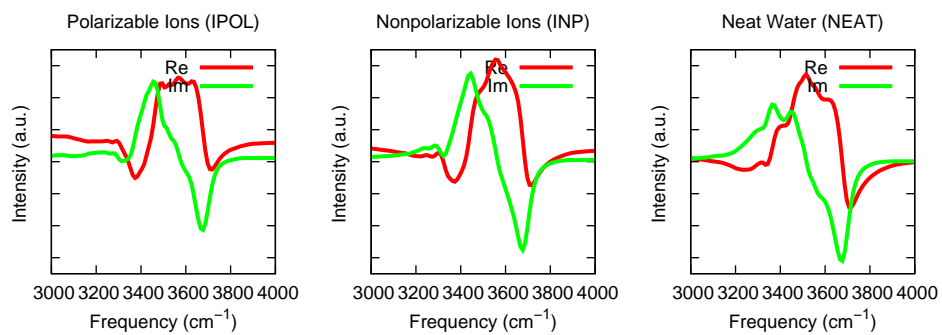


Figure 8: Theoretical resonant susceptibilities ( $\chi_{xxz}$ ,  $\chi_{yyz}$ ) of IPOL (left panel), INP (center panel), and NEAT (right panel).

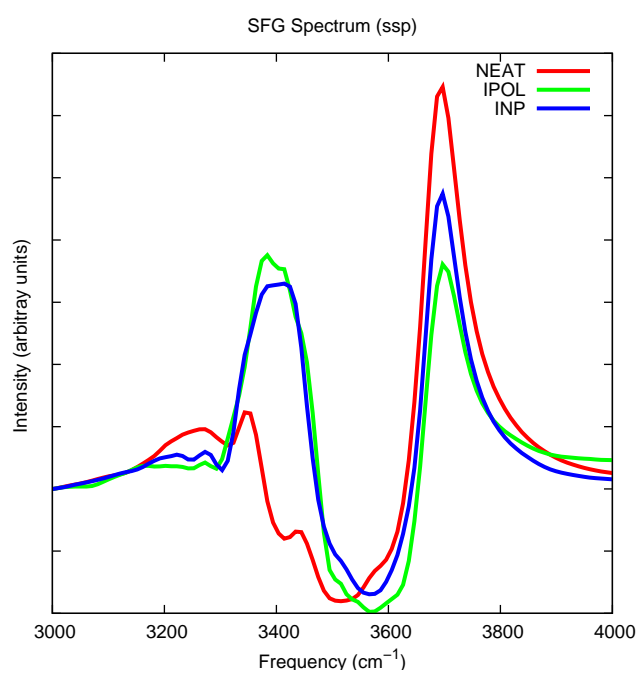


Figure 9: Theoretical vibrational Sum Frequency Generation spectrum (ssp) of IPOL, INP, and NEAT.